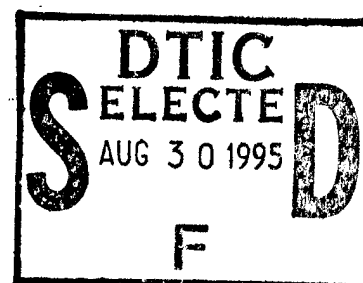AD_____

MIPR NO: 94MM4539

TITLE: Crystal Diffraction Spectrometry for Accurate, Non-Invasive kV/
        Spectral Measurement for Improvement of Mammographic Image Quality

PRINCIPAL INVESTIGATOR:
    Primary: Richard D. Deslattes
    Alternate: Larry Hudson

CONTRACTING ORGANIZATION:
    Physics Laboratory
    National Institute of Standards and Technology

REPORT DATE: April 30, 1995

TYPE OF REPORT: Annual

PREPARED FOR: U.S. Army Medical Research and Materiel
                Command
                Fort Detrick, Maryland 21702-5012

DISTRIBUTION STATEMENT: Approved for public release;
                          distribution unlimited

The views, opinions and/or findings contained in this report are
those of the author(s) and should not be construed as an official
Department of the Army position, policy or decision unless so
designated by other documentation.

19950703 035

DISCLAIMER NOTICE
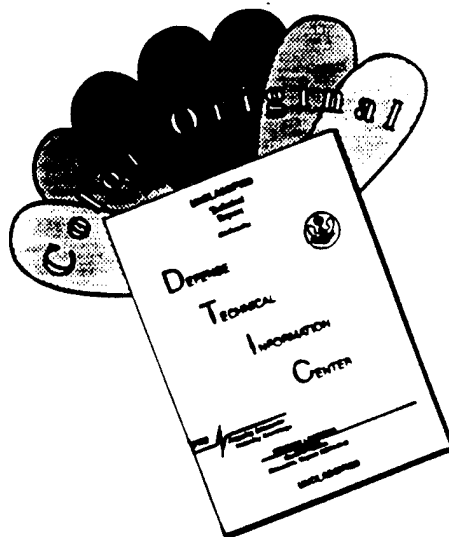
THIS DOCUMENT IS BEST QUALITY AVAILABLE. THE COPY FURNISHED TO DTIC CONTAINED A SIGNIFICANT NUMBER OF COLOR PAGES WHICH DO NOT REPRODUCE LEGIBLY ON BLACK AND WHITE MICROFICHE.

REPORT DOCUMENTATION PAGE

1. AGENCY USE ONLY (Leave blank)	2. REPORT DATE 30 Apr 95	3. REPORT TYPE AND DATES COVERED Annual 18 Apr 94 – 31 Mar 95

4. TITLE AND SUBTITLE

Crystal Diffraction Spectrometry for Accurate, Non-Ivasive kV/Spectral Measurement for Improvement of Mammographic Image Quality

5. FUNDING NUMBERS

94MM4539

6. AUTHOR(S)

Richard Deslattes
Larry Hudson

7. PERFORMING ORGANIZATION NAME(S) AND ADDRESS(ES)

National Institutes of Standards and Technology
Gaithersburg, Maryland 20899

8. PERFORMING ORGANIZATION REPORT NUMBER

9. SPONSORING / MONITORING AGENCY NAME(S) AND ADDRESS(ES)

U.S. Army Medical Research and Materiel Command
Fort Detrick, Maryland 21702-5012

10. SPONSORING / MONITORING AGENCY REPORT NUMBER

11. SUPPLEMENTARY NOTES

12a. DISTRIBUTION / AVAILABILITY STATEMENT

Approved for public release; distribution unlimited

12b. DISTRIBUTION CODE

13. ABSTRACT (Maximum 200 words)

Phase one of this contract has been devoted to the development and demonstration of the NIST prototype crystal spectrometer which was designed to provide accurate measurement of x-ray source voltage and full spectral characterization of the radiation emitted from mammographic x-ray sources. A major advance has been the movement from film to solid state image registration. Our current systems take advantage of recently introduced large area digital radiography sensors which are now being used in place of dental film. Initial clinical trials indicated the need for improved detection quantum efficiency. This has been overcome primarily by increasing the crystal bandpass with an air abrasive treatment of the surface and retrofitting the sensor with a thicker scintillating material. The significance of these advances is that we now have an instrument which: measures kVp to an accuracy in excess of clinical requirements, is easily adaptable to the clinical setting, records the entire spectral profile, including the effects of both inherent and added filtration, and is sensitive enough to obtain these data within the time of a typical mammographic exposure. Not only will this contribute to the quality control of mammography but potentially to refinements in technique.

14. SUBJECT TERMS

15. NUMBER OF PAGES 23

16. PRICE CODE

17. SECURITY CLASSIFICATION OF REPORT	18. SECURITY CLASSIFICATION OF THIS PAGE	19. SECURITY CLASSIFICATION OF ABSTRACT	20. LIMITATION OF ABSTRACT
Unclassified	Unclassified	Unclassified	Unlimited

FOREWORD

Opinions, interpretations, conclusions and recommendations are those of the author and are not necessarily endorsed by the US Army.

_____ Where copyrighted material is quoted, permission has been obtained to use such material.

_____ Where material from documents designated for limited distribution is quoted, permission has been obtained to use the material.

RDD Citations of commercial organizations and trade names in this report do not constitute an official Department of Army endorsement or approval of the products or services of these organizations.

_____ In conducting research using animals, the investigator(s) adhered to the "Guide for the Care and Use of Laboratory Animals," prepared by the Committee on Care and Use of Laboratory Animals of the Institute of Laboratory Resources, National Research Council (NIH Publication No. 86-23, Revised 1985).

RDD For the protection of human subjects, the investigator(s) adhered to policies of applicable Federal Law 45 CFR 46.

_____ In conducting research utilizing recombinant DNA technology, the investigator(s) adhered to current guidelines promulgated by the National Institutes of Health.

_____ In the conduct of research utilizing recombinant DNA, the investigator(s) adhered to the NIH Guidelines for Research Involving Recombinant DNA Molecules.

_____ In the conduct of research involving hazardous organisms, the investigator(s) adhered to the CDC-NIH Guide for Biosafety in Microbiological and Biomedical Laboratories.

Accesion For		
NTIS CRA&I	☑	
DTIC TAB	☐	
Unannounced	☐	
Justification		
By _____		
Distribution /		
Availability Codes		
Dist	Avail and / or Special	
A-1		

PI - Signature   4/14/95

                                                    Date

TABLE OF CONTENTS

Introduction

Nature of the Problem. This work was motivated by the well established sensitivity of mammographic image quality to the high voltage (kV) applied to the x-ray source. Clinical experience indicates that changes as small as 1 kV are significant [1]. Less frequently discussed, though also clearly important, is the overall spectral distribution of the radiation delivered to the patient. Recent work in the Physics Laboratory at the National Institute of Standards and Technology (NIST), has resulted in prototype instruments based on (Bragg-Laue) crystal diffraction to gain accurate measurement of x-ray source voltage and full spectral characterization of the emitted radiation [2]. The approaches to kV standardization used prior to the recent NIST work in the mammographic region possess inherent limitations. As described in detail in our original proposal, these approaches include traditional invasive high voltage dividers as well as non-invasive filtration and fluorescence threshold methods. In an effort to overcome the limitations of previously available methods, we have demonstrated the effectiveness of a particular form of wavelength-dispersive crystal diffraction spectrometry. This method has high intrinsic precision and accuracy; it is self-calibrating and capable of acquiring spectral data in parallel at arbitrarily high rates, permitting its application to clinical sources operated at full power. This new technology obviates the need for invasive electrical measurements, overcomes the limitations inherent in filtration and fluorescence threshold methods, and has produced results whose accuracy exceeds clinical requirements.

Aside from its accuracy and its adaptability to the clinical setting, the NIST spectrometric procedure gives not only the high energy limit of the continuous x-ray spectrum (which is numerically equal to the voltage applied to the x-ray source) but also the entire spectral profile, including the effects of both inherent and added filtration [2]. This capability invites potentially more discerning studies of the variation of image quality as a function of deliberately introduced changes in the overall spectral distribution. A further use of this overall spectral information is to detect target deterioration due to the transport of filament material (tungsten) and of the cathode support structure (frequently nickel). Such processes occur naturally over the long term even with conservative operation of an x-ray source and much more rapidly with less careful operation. It is at least plausible that such spectral degradation should effect diagnostic efficiency, as will be investigated.

Background of previous work. To demonstrate the practicality of this approach, we first built a small spectrograph using symmetric Laue diffraction according to a format introduced early in this century by Rutherford and Andrade [3]. The original prototype spectrometer and experimental arrangement is illustrated in Fig. 1. It shows a small focal spot x-ray source, a diffraction crystal (originally employing the silicon [220] reflection in a flat crystal geometry), an intermediary aperture and an image registration plane, illustrated as x-ray sensitive film. Although the absolute lattice parameter of the crystal is accurately known in terms of the fundamental standards, it is not a necessary input since emission and/or absorption features in the spectra are otherwise known with an accuracy of the order of 10 ppm or better. Such information provides an internal calibration for the pattern of images seen on a film or other imaging detector.

An example of a densitometer trace for a film exposed in the device illustrated in Fig. 1 is shown in Fig. 2. Note that each spectral feature is duplicated, once on a leftward oriented dispersion curve

and once rightward. This mirror-symmetric duplication eliminates the troublesome question of where the recorded spectrum begins. The following figure, Fig. 3, shows an expanded view of the region near the end-point energy. The intersection between the indicated background and the linearly varying continuum distribution, which gives the accelerating potential applied to the x-ray source, is clearly discernable with an imprecision of 0.1 kV, a level of refinement that exceeds the needs of mammographic practice as they are currently understood. Should further refinement be needed, it is straightforward to achieve 10 V accuracy by simple modifications of the apparatus.

In more recent work (as yet unpublished) we have addressed an important limitation of the flat crystal x-ray optics illustrated in Fig. 1, namely its dependence on focal spot size. Specifically, resolution (and hence voltage precision) depends on the x-ray focal spot size which, though adequate in newer sources, is highly variable among older installations. To circumvent this limitation, we have begun to make use of the focussing crystal optics illustrated in Fig. 4. This geometrical change entails several consequences among which are: enhanced spectral dispersion so that a Si [111] crystal provides dispersion equal to that of the Si [220] flat crystal which had proven adequate, the combined effects of the larger structure factor for Si [111], and finally the focussing action of the curved crystal significantly increases the efficiency of the spectrometer.

Purpose of the Present Work.
(1) To move from film to solid state image registration:
A more desirable modality for use in the field would make use of electronic imaging technology interfaced to a portable computer. The main direction of this work is toward use of available phosphors, CCD's and image acquisition and analysis software.

(2) To increase the detection quantum efficiency (DQE) of the device:
The narrow diffraction widths (~ 1-2 eV) of perfect crystals used in the original prototype imply a considerable loss in x-ray sensitivity relative to a more optimally matched window with a width of about 100 eV. As a remedy, we are by various means trying to introduce a deliberate gradient in the crystal's interplanar spacing whose effect should be to increase the acceptance bandwidth and hence the instrument's efficiency. Modifications of the sensor itself and phosphor conversion layer are also being investigated to enhance the DQE.

(3) To perform clinical studies:
Our primary goal, in collaboration with various groups, is to demonstrate the applicability and ease of use of this new device in a clinical setting to calibrate the high energy applied to mammographic x-ray sources. Secondary goals relate to taking advantage of the full spectral characterization available. With this device, it is now possible to study new target and filter combinations, and from existing clinical installations of varying ages, operating modalities and histories. Specifically, there are two main issues that could be explored: (i) First it is conjectured that the full spectral characterization of test systems including conventional and novel x-ray sources with an extended range of filtration options will lead to either improved technique outside of the presently considered parameter space or to an appreciation that the present range of source and filter combinations is already optimal. (ii) Second, it is proposed that spectra produced in the cohort of x-ray tubes currently in clinical use may not be adequately represented by their nominal anode composition at the time of manufacture. If this spectral variability is, in fact, encountered, then it will be of considerable interest to determine the extent to which these changes influence diagnostic efficacy (at the level of phantom-based scoring procedures).

3

Methods of approach.

Crystal preparation, spectrometer manufacture, evaluation of imagers, and the development and testing of advanced prototypical systems are conducted within the Physics Laboratory of NIST.

The range of needed clinical studies and the qualified personnel required are outside the scope of the technical development program at NIST. Accordingly, on the basis of initial expressions of interest by several clinically based groups, a letter was circulated suggesting the formation of a loose coalition of such investigations, all of which would be given access to prototype instrumentation from the NIST program. The first partnership has been established with the Center for Devices and Radiological Health (CDRH) in the FDA's Rockville laboratories. The initial clinical collaborations include: Georgetown University Medical Center, Massachusetts General Hospital, the University of Alabama Medical Center, the University of California, Davis, the University of Washington, Seattle and the University of Wisconsin, Madison. The general idea is to facilitate rapid, parallel investigation along the main coordinates in the parameter space associated with physical source characteristics.

One example of planned studies is the approved thesis research program of Ms. Catalina Barss (Georgetown University). Using a NIST spectrometric device, she plans to obtain spectra and kV calibration data from several clinics in the Washington metropolitan area. The sources chosen for study will be widely dispersed in age and operating history, allowing her to evaluate the extent to which spectra reflect nominal target composition through the aging process.

Experimental Methods and Results of Present Work

The first year of this grant has supported initial tests with a clinical x-ray source as well as a number of critical developmental improvements of the spectrometer/detection system. They were primarily aimed at increasing the quantum detection efficiency of the system and packaging the device so as to be compact and portable. The advances and rationale are described individually below. They include:

(1) Utilization of an inexpensive scheme of digital registration of spectral images.
(2) Increase of the gain of the adc's of the image acquisition electronics.
(3) Modification of the dimensions of the spectrometer body to match the CCD sensor.
(4) Introduction of a pinhole camera along the center axis of the spectrometer.
(5) Subtraction of thermal background from CCD images.
(6) Initial clinical studies.
(7) Comparison of elastically bendable crystal materials for high x-ray reflectivity.
(8) Increase of the crystal bandpass with an air abrasive treatment of the surface.
(9) Retrofitting of the sensor with a thicker scintillating material.
(10) Mounting of the spectrometer in a positioning device; packaging a compact and portable system.
(11) Derivation of analytic, parametric equations for the curved crystal wavelength dispersion function in Cauchois geometry.

While almost all forms of direct electronic x-ray imaging are, in principle, applicable to the current problem of spectral registration, the need for a simple, low cost system with adequate sensitivity led fairly rapidly to a focus on optical charge coupled devices (CCD's) with phosphor conversion layers. We considered both the use of fiber optic tapers with minification to small (low cost) CCD's and direct (1:1) use larger format imagers.

Our current systems take advantage of recently introduced large area digital radiography sensors which are now being used in place of dental film. Because of the logarithmic response of photographic film, these CCD-based sensors do not possess comparable dynamic range but they do possess greater sensitivity and contrast. In the present work we use a size 2 dental sensor from Schick Technologies, Inc.[4] It has an active area of 36.5 x 25.2 mm and is comprised of 760 x 524 square pixels 48μm on a side. It is packaged in an anodized aluminum case as a 6 mm thick sandwich consisting of a scintillator, fiber optic faceplate, CCD and I/O cable. The sensor is supported by a drive electronics module and power supply which is connected in turn to a PC-based 8-bit ISA bus interface card. Software is provided that can capture 12-bit images for a user-specified amount of time at a spatial resolution of 9-10 lp/mm. This type of a system is rendered economical by of the use of a biasing scheme which greatly suppresses the collection of dark current providing high signal to noise at room temperature without the requirement of active cooling.

Dental x-ray sources are intense relative to our application and generally operated around 70 keV. To increase the sensitivity, we increased the system gain by a factor of five by replacing a resistor in the drive electronics module. In this configuration one sees a modest thermal background grow in during the few seconds of a typical measurement using one of our low-current laboratory x-ray sources. This modest "fogging" as well as artifacts due to point defects in the CCD are largely offset by image subtraction of a dark image acquired with the same time as the exposed image. The only further image processing we perform is a column sum (or projection) of the vertical spectrum to obtain a one-dimensional spectrum for further analysis. The spectrometer body was modified to match the dimensions of the CCD size-2 dental sensor. The radius of curvature was decreased to 15.2 cm (6 in.) to reduce the lateral image extent and the height of body cavity was increased to take advantage of the 25.2 mm height of the sensor. A schematic of our most recent, 6-inch prototype is shown in Figure 4. A two-dimensional color image acquired with this spectrometer and digital sensor is shown in the top portion of Figure 5. A background (dark) image has been subtracted. The spectrometer used a Si(111) crystal of 185μm thickness. In the center, one sees the structure of the focal spot of the x-ray source imaged by a pin-hole camera which is on the center axis of the spectrometer. The pinhole is in the center of the faceplate and estimated to be about 10 μm diameter. The column-summed profile of these data are shown in bottom of Figure 5.

The effectiveness of thermal background subtraction is shown in Figure 6. This was acquired with one of our low-current laboratory x-ray sources for a period of about 54 s so the thermal background is much higher than would be experienced in a clinical setting. This spectrum was taken at a source voltage of 22 kV and with 25 μm of Mo filtration.

In September 1994 the prototype spectrometer described above was taken to the Rockville laboratory of the FDA's Center for Devices and Radiological Health (CDRH) for a field trial with a mammographic x-ray source. Results were promising until a 30μm Mo filter was inserted into

the incident x-ray beam. The effect of the loss in signal (Figure 7) due to absorption in the filter raised concern over the increase in uncertainty over the position of the high-energy cutoff. This becomes increasingly important at lower energies because the x-ray source emits much less x-ray flux. Since many field mammographic sources contain permanently mounted filtration, we were motivated to undertake further development to increase the sensitivity of the device, even at the cost of some loss of spatial resolution.

We tested several other crystals [Ge(111), PET(020), LiF(200)] which could be both cut so as to provide a high-reflectivity plane in transmission and also bent elastically to a small radius of curvature without breaking. The only one which proved to be brighter than Si(111) was LiF(200). For example, a 500µm thick LiF(002) reflected about seven times more 28 keV light than a 185 µm thick Si(111). Unfortunately, the crystalline quality of commercial available LiF is poor and spectral lines are smeared. X-ray topography revealed multiple domains in our fusion-grown LiF crystal. The d-spacing of LiF(200) would also require a heat-treatment to bend LiF to the 10.2 cm radius of curvature required to focus the image onto a size 2 dental sensor. We also plan to try the bright (101) reflection of quartz.

We then attempted to introduce a strain gradient near the surface of a silicon crystal which would increase its bandpass. Rouge polishing proved ineffectual. In marked contrast, the application of an air abrasive treatment using fine aluminum oxide grit produced about a factor of two of increased throughput. The effect was reproducible and quickly saturated after producing a frosted appearance on the surface. Work is now underway to obtain crystals which have defects distributed throughout the bulk which might enhance throughput even further.

A final breakthrough, which raises the system sensitivity to a commercially viable and attractive level, was achieved by retrofitting the dental sensor, replacing the deposited 100 µm thick scintillating layer with a Lanex Regular mammography screen (150 µm of Gd_2O_2S plus dopants). The increase was about a factor of three with higher energies gaining more than lower energies. The resolution of the sensor went from 9-10 lp/mm to about 6 lp/mm. The relative gain in sensitivity due to the combined effect of crystal treatment and sensor modification is illustrated in Figure 8. The plot shows two spectra acquired with the same Si(111) crystal curved to 15.2 cm and spectrometer, the same Mo x-ray tube (150 µm focal spot), and the same experimental conditions (30 kV, 1.4 mA, and only 16 mA-s). The differences in the upper curve are due to submitting the crystal surface to an air abrasive treatment (increasing the signal a factor of 2), retrofitting the CCD dental sensor to include a mammography screen as the convertor to visible (contributing an additional factor of two to three depending upon energy), and finally subtracting a background image to eliminate most of the noise due to thermal background. While the two spectra have offset zeroes, they are on the same relative scale.

These gains in sensitivity position us to resume field testing of the spectrometer system in the final phase of this work. We now expect to be able to acquire suitable spectra from filtrated sources within the time of a standard clinical mammographic exposure. Indeed, the data in Figure 6 were taken using our most advanced prototype under the "worst case" conditions of low HV (22 kV) and 25 µm molybdenum filtration.

Improvements have also been made in the areas of packaging and mounting. During our initial

Improvements have also been made in the areas of packaging and mounting. During our initial tests with a clinical x-ray source at the FDA, we transported a full-sized computer and monitor. This is impractical for *e.g.* the roving health inspector. The present system consists of a low cost notebook computer and docking station. The docking station holds the CCD interface card in an ISA bus. The two pieces fit conveniently in a normally sized brief case. Future configuration might include a one-piece "lunchbox" computer with ISA bus or a notebook with PC-MCIA interface. The spectrometer itself is now mounted with two degrees of freedom. It's height may be adjusted after positioning it on the standard mammographic plate. It is also supported in a cradle which allows adjustment of the tilt angle accepting the entrance beam. The cradle is equipped with a handle so the spectrometer and stowed cabling may be carried in one hand while the encased computer occupies the other.

The supplier of the dental CCD system has modified their data acquisition software to compute a column sum from a two-dimensional image, producing the spectrum of interest. Additional software is being developed in-house which will extract a high-energy cutoff from an input spectrum. The theoretical plate-function for a curved crystal in Cauchois geometry has been derived with the assistance of the tools in the commercial software package Mathematica. This function establishes the connection between distance and energy along the dispersion axis of the CCD. The resulting plate function which is analytic and parametric is shown in Appendix 1.

Conclusions

Three goals are outlined above in the Introduction under the heading Purpose of the Present Work. In their abbreviated form they are:
    (1) To move from film to solid state image registration.
    (2) To increase the system detector quantum efficiency.
    (3) To perform clinical studies—first proof of principle and then other studies which use the availability of the full spectral characterization.

As outlined above under Results, the first phase of this work has seen the successful completion of goals 1 and 2 as well as initial studies with a clinical mammographic x-ray source. Clearly the balance of this project will be focused on acquisition and analysis of data acquired at various clinical settings. These venues have been described in detail under Methods of Approach in the Introduction. These studies promise to be informative, interesting, and may potentially contribute to an improved paradigm in the acquisition of mammograms.

Figure Captions

Fig. 1 Diagram of an early flat-crystal prototype instrument for determining both end point energies and overall spectral distributions.

Fig. 2 Typical densitometer tracing from a film exposed in the spectrometric apparatus of Fig. 1. The needed energy scale can be established either by length metrology or by referring to the well established energy values for the characteristic x-ray lines or edges shown.

Fig. 3 An expanded view of densitometric measurements near the end-point energy (numerically equal to the kilovoltage applied to the x-ray tube). Here, refinement is clearly of the order of 0.1 kV.

Fig. 4 Schematic diagram of a curved crystal modification of the spectrometric device shown in Fig. 1. In the curved crystal arrangement shown, the spectroscopic resolution realized is entirely independent of focal spot size. The crystal radius of curvature (distance from crystal to image plane) is six inches.

Fig. 5 Top: False color image from the spectrometer shown in Figure 4 acquired with the dental CCD described in the text. A pinhole-camera image of the focal spot is visible in the center of the image. Bottom: The log of the column sum of the image shown above. This shows the molybdenum spectrum (the alpha lines are saturated) with high-energy cutoff and, in the center, the focal spot.

Fig. 6 Demonstration of the effectiveness of thermal background subtraction in revealing the high-energy cutoff. This is a long-duration exposure (54 s) and therefore extreme example.

Fig. 7 Results from initial clinical studies. The high-energy cutoff was difficult to discern in this early prototype under Mo filtration. This motivated the production of advanced prototypes with enhanced sensitivity.

Fig. 8 The relative improvement attained from both a surface treatment of the diffracting crystal and the retrofitting of the phosphor conversion layer of the CCD sensor.
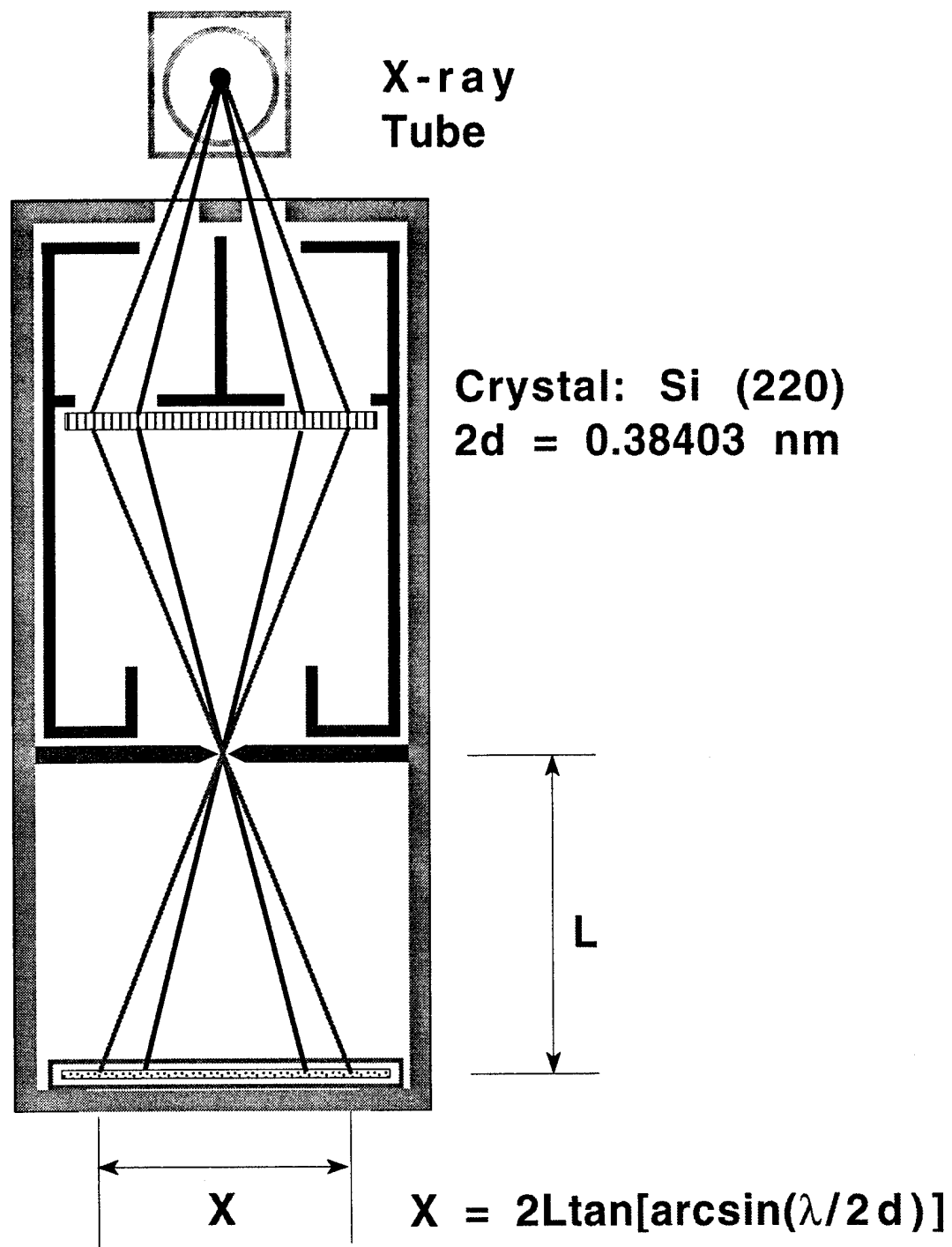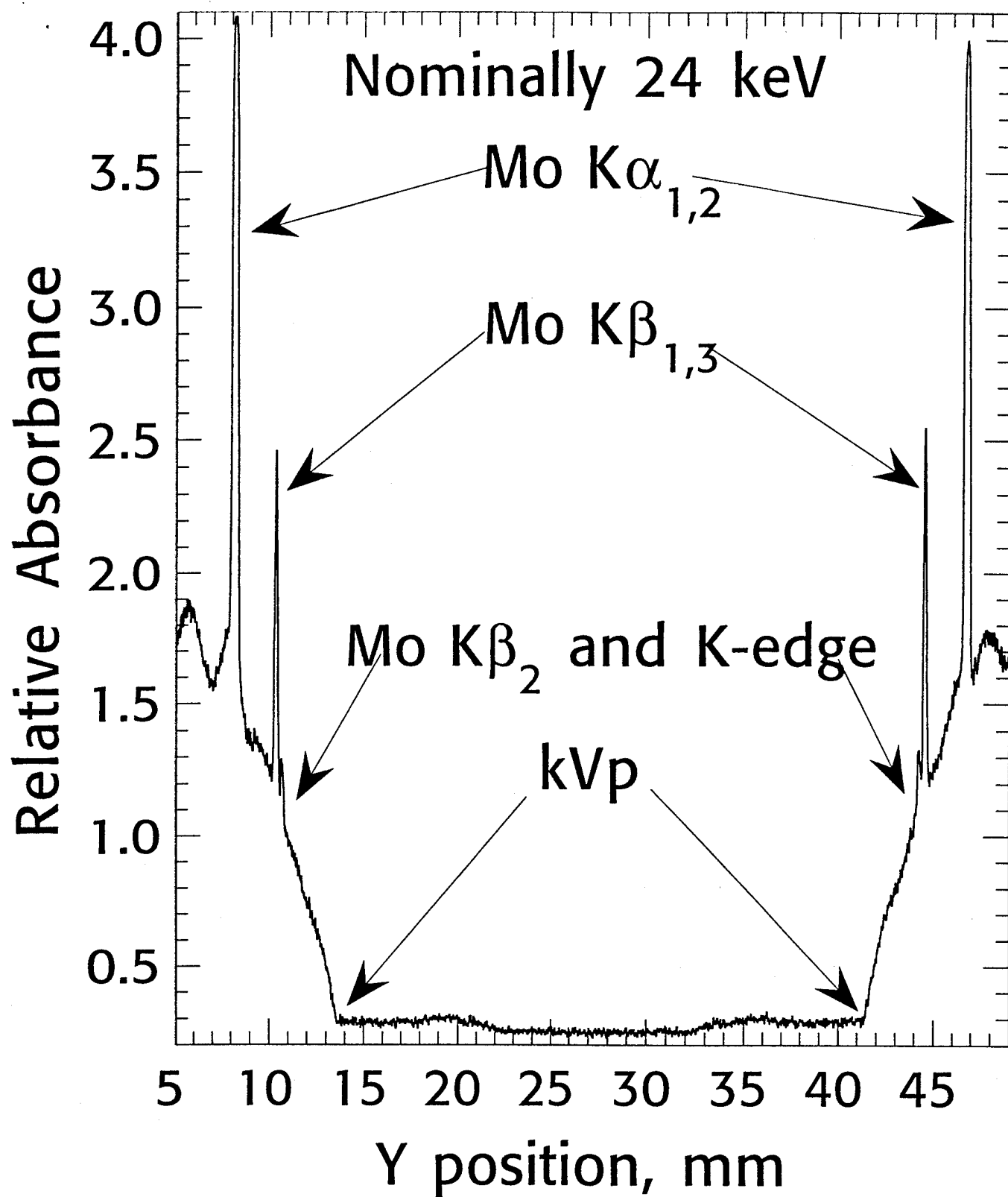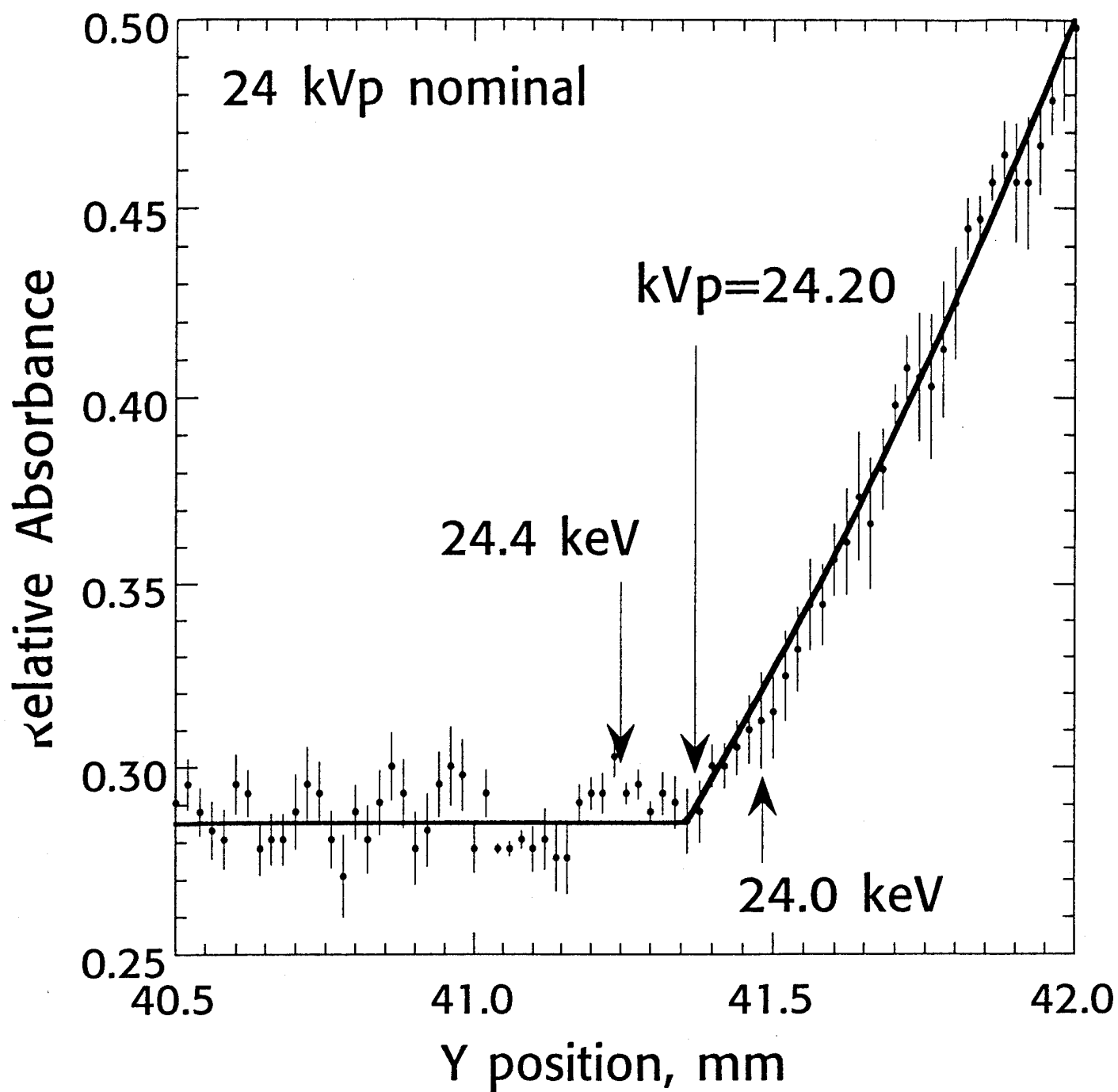
X-ray
Tube

Crystal: Si (220)
2d = 0.38403 nm

L

X

$X = 2L\tan[\arcsin(\lambda/2d)]$

FIGURE 1

9

FIGURE 2

10

FIGURE 3

//

X-RAY SOURCE

CURVED CRYSTAL

SCATTER BAFFLE

CCD SENSOR

FIGURE 4

16
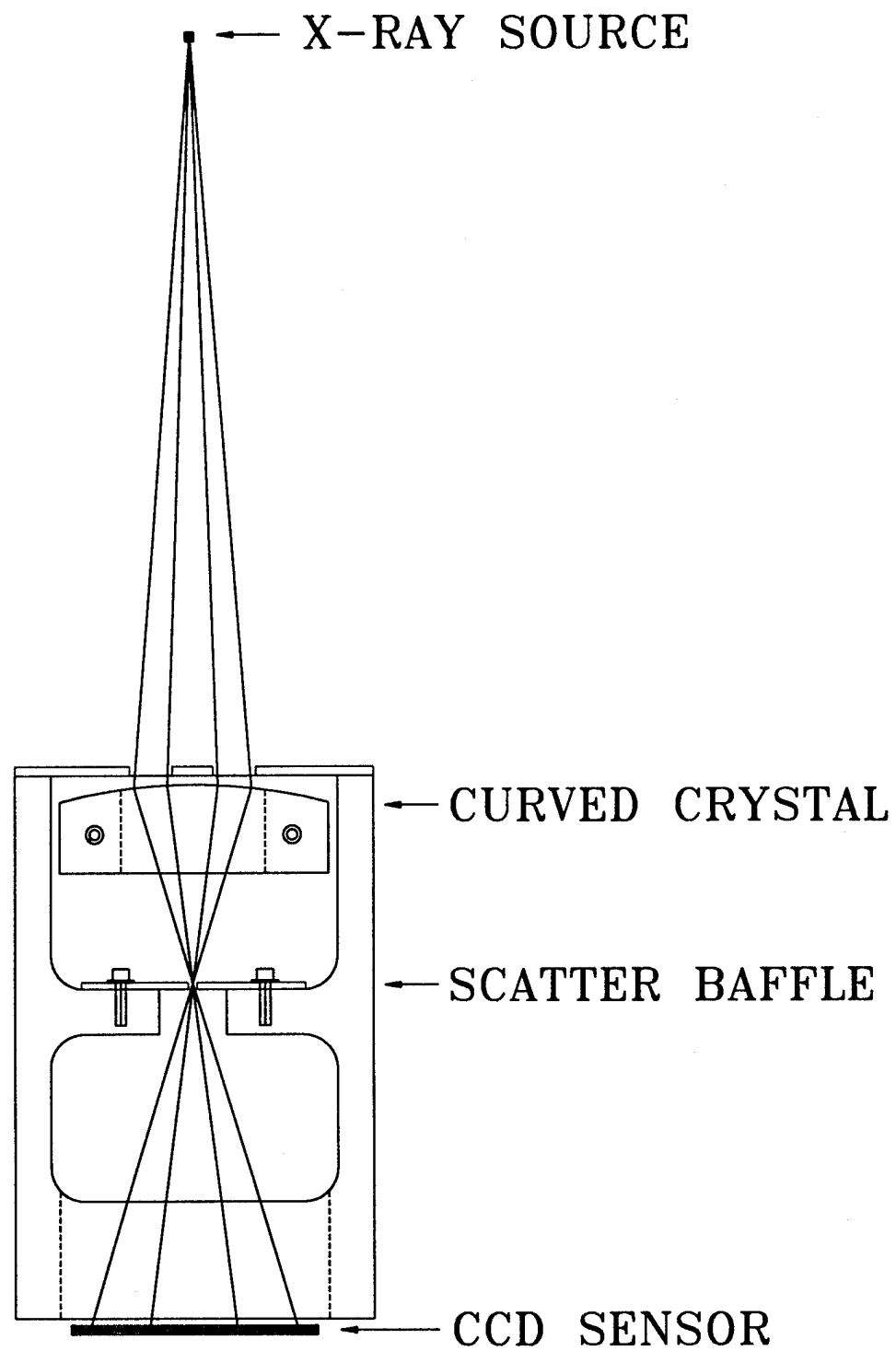
X-ray Spectral Image From Dental CCD

FIGURE 5

13

22kV, 2.5mA, 134mA-s, 25um Mo filtration, Si(111)

Pixel Column Sum

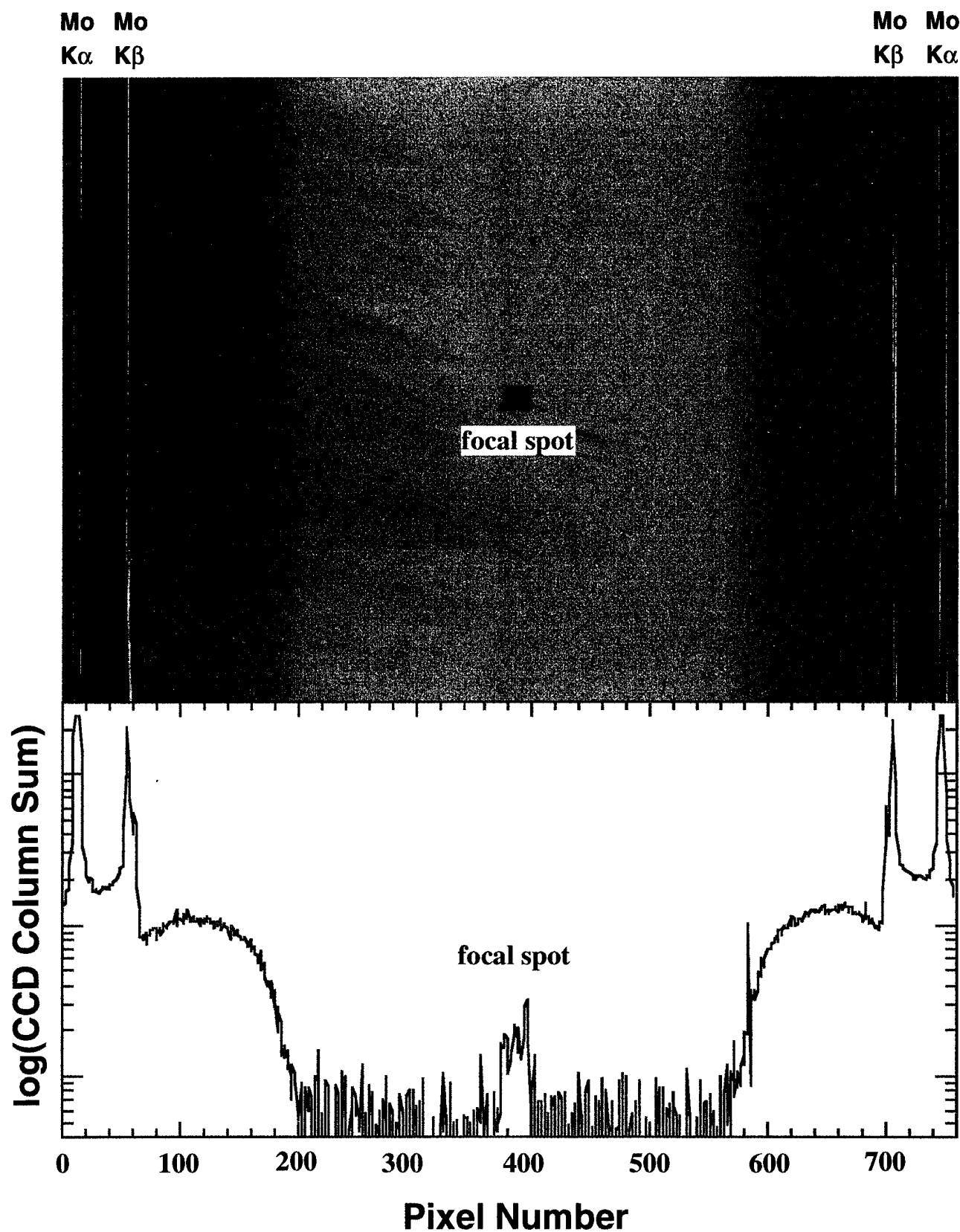Signal (offset)

Background

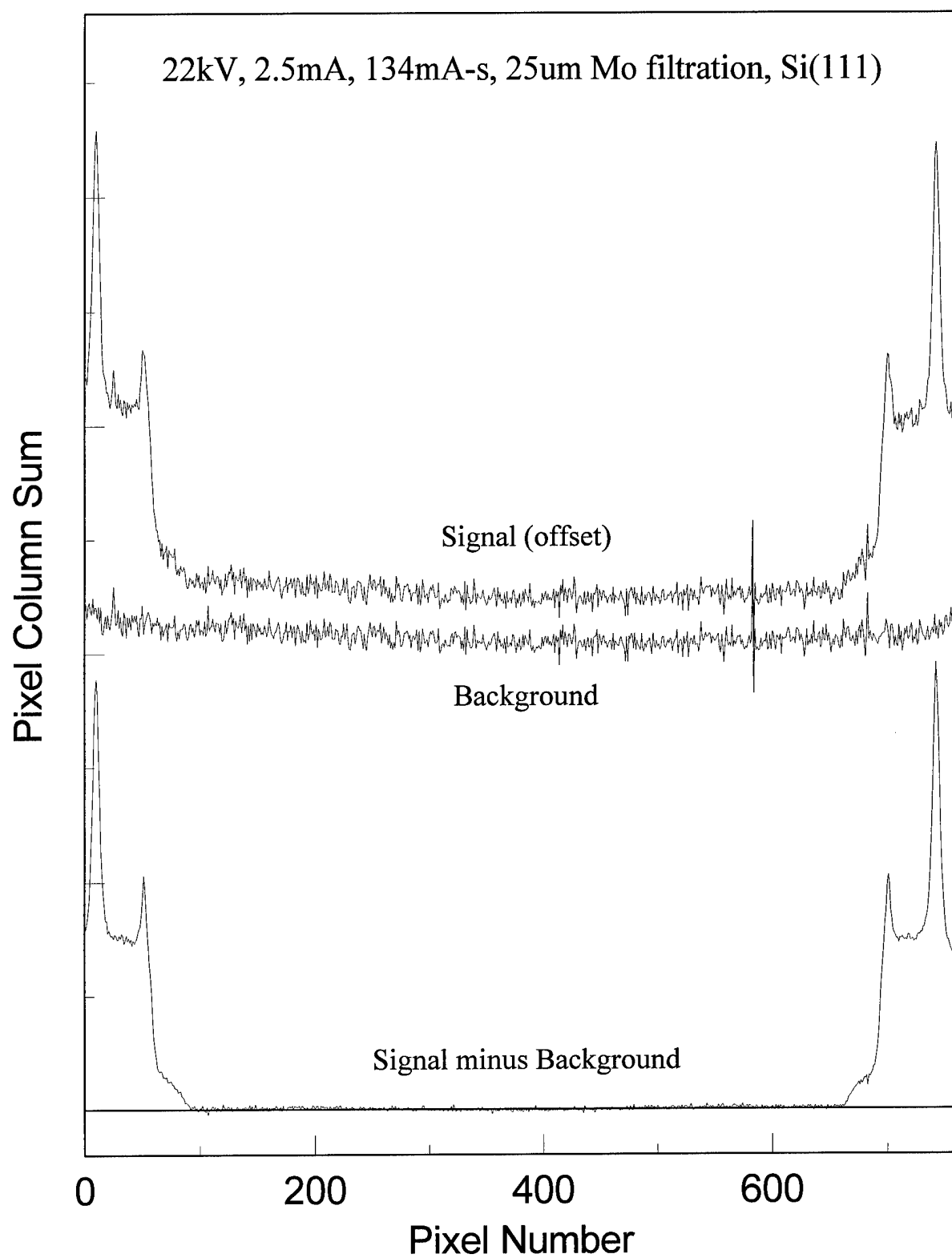Signal minus Background

Pixel Number

Figure 6

14

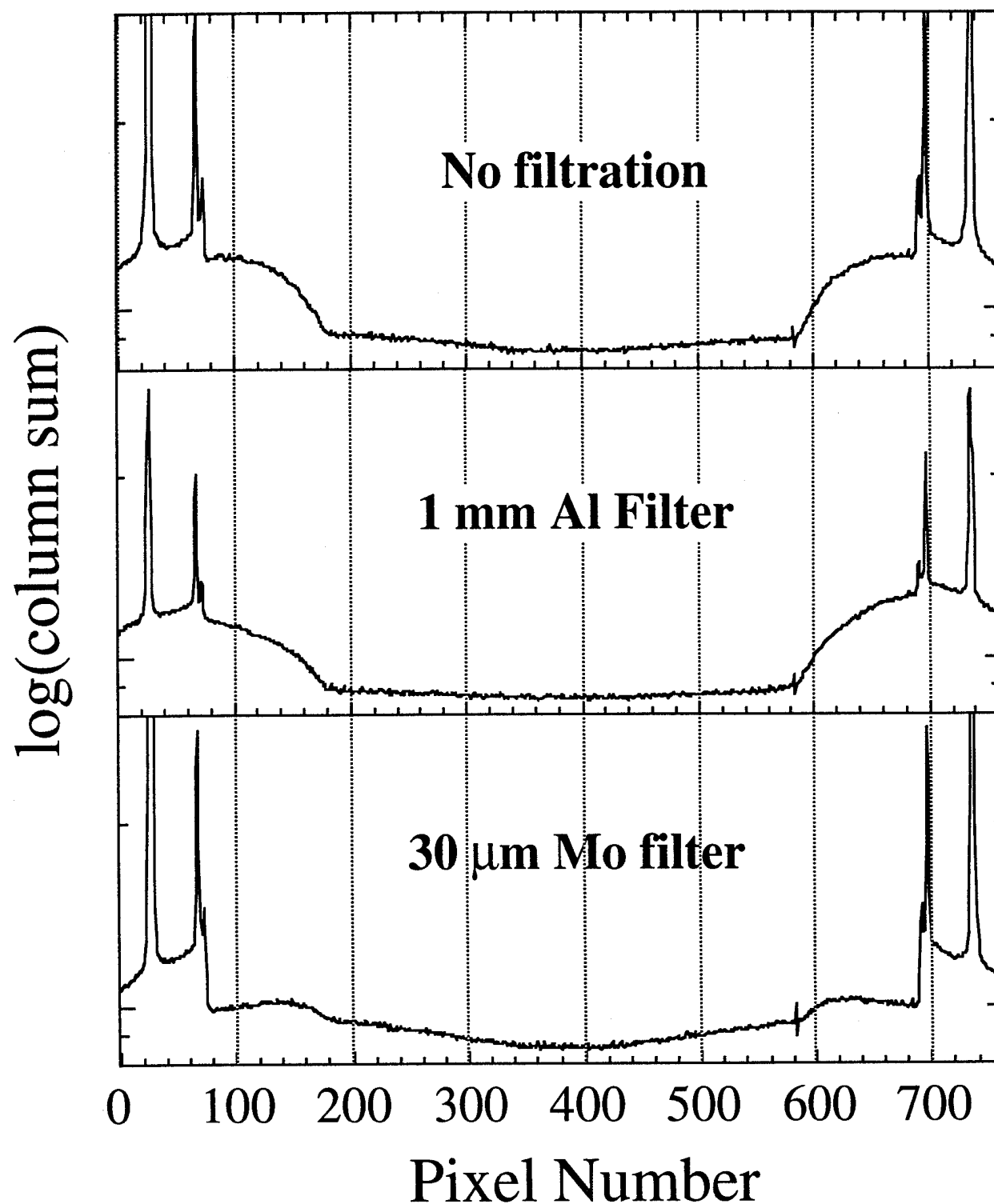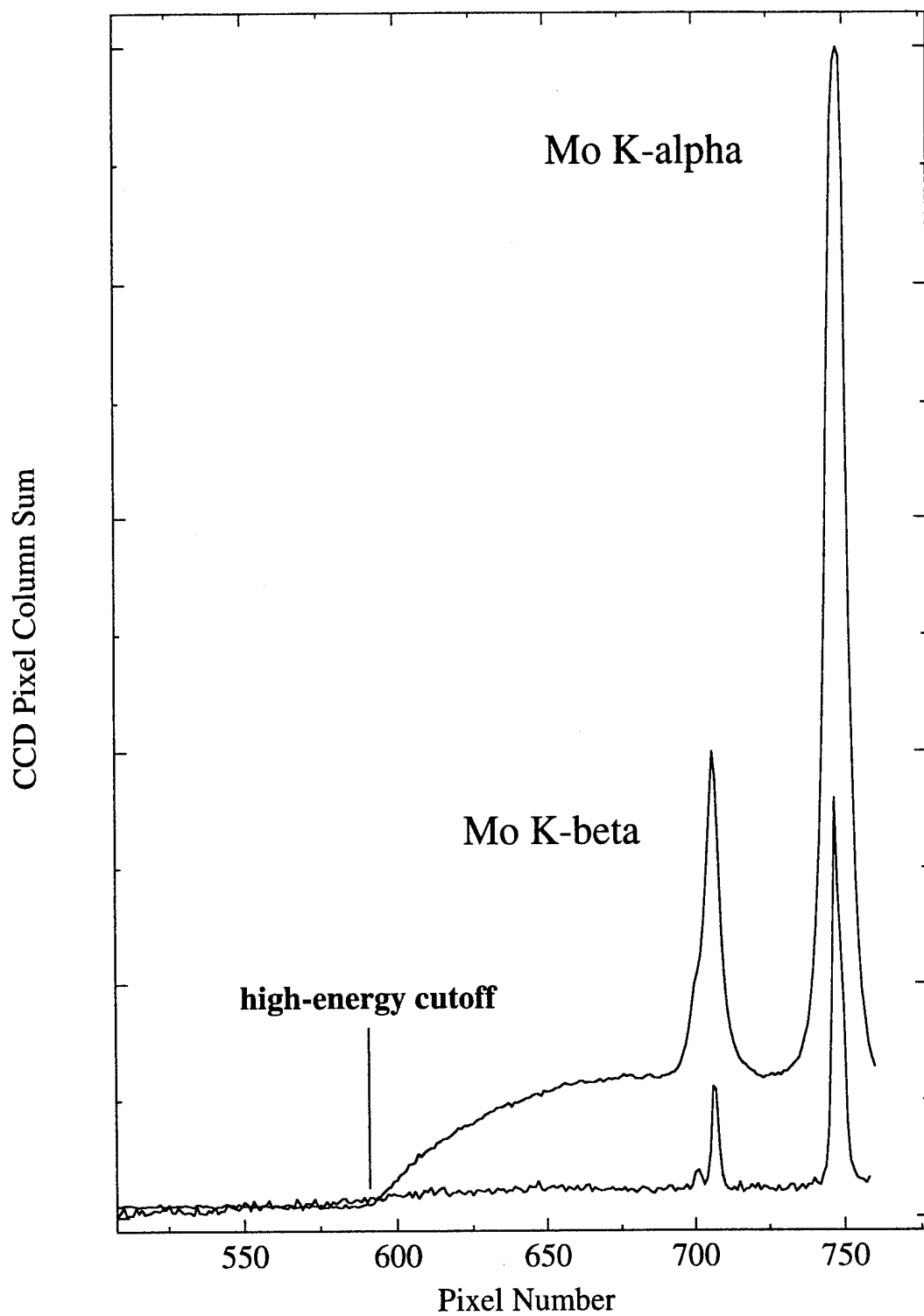320 mA-s, 30 kV, Mo Anode, 0.3x0.3mm spotsize
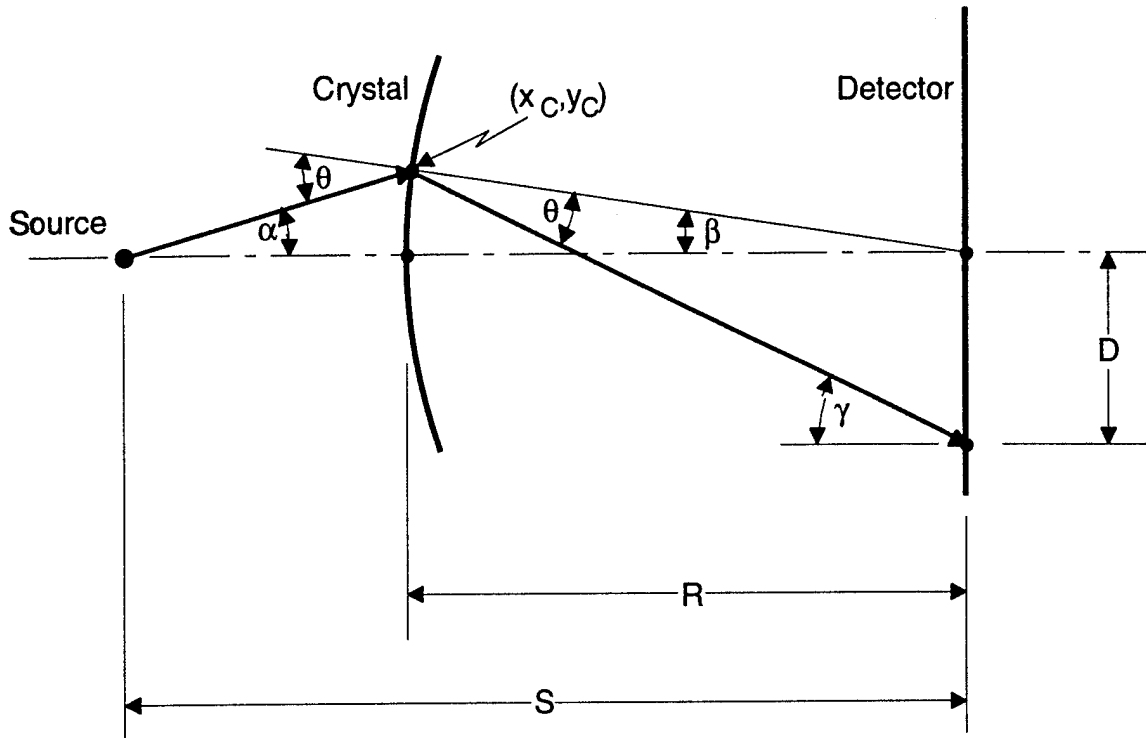

FIGURE 7

FIGURE 8

16

References

[1]   J. Law, K. Faulkner and S. Smith, "Variation of image quality with x-ray tube potential in mammography," Br. J. Radiol. **62**, 192-194 (1989); J. Law, "The measurement and routine checking of mammography x-ray tube kV," Phys. Med. Biol. **36**, 1133-1139 (1991).

[2]   R. D. Deslattes, J. C. Levin, M. D. Walker, and A. Henins, "Crystal diffraction spectrometry for non-invasive high voltage measurement in mammography," Medical Physics, in press.

[3]   E. Rutherford and E. N. da C. Andrade, "The spectrum of the penetrating x- rays from Radium B and Radium C," Phil. Mag. **28**, 263-273 (1914); ibid., "The wavelength of the soft x-rays from Radium B," **17**, 854-868.

[4]   This does not constitute an endorsement by the United States Government but is given as a matter of information.

**An Analytic, Parametric Treatment of the
Curved-Crystal Plate Function for Cauchois Geometry**

As shown in the figure, the crystal has a radius of curvature R. The detector is located at the center of curvature of the crystal and the source is located a distance S away from the center of curvature along a perpendicular to the detector. Consider photon emission only in the plane of the figure, *i.e.* assume the crystal has zero height. Let α be the emision angle of the photon from the source with respect to the perpendicular from the detector. The photon strikes the crystal at the point (x_C, y_C) given by:

$$x_c = -\left(S\tan^2\alpha + A\right)\cos^2\alpha$$
$$y_c = (S-A)\cos\alpha\sin\alpha$$

where A is defined by

$$A \equiv \sqrt{R^2 + \left(R^2 - S^2\right)\tan^2\alpha}.$$

The Bragg angle θ is given by

$$\theta \equiv \theta_{\text{Bragg}} = \alpha + \beta$$

where the angle β is:

$$\beta \equiv \tan^{-1}\left(-y_C/x_C\right) = \tan^{-1}\left[\frac{(S-A)\tan\alpha}{A + S\tan^2\alpha}\right].$$

Then the energy E of the photon that will be Bragg refracted is given in terms of α by

18

$$E = \frac{\Lambda}{\lambda} = \frac{n\Lambda}{2d\sin\theta}$$

where λ = wavelength, d = crystal lattice spacing, n = order of refraction, and the energy-wavelength conversion constant $\Lambda = hc = 1.23984244$ nm·keV. The distance D from the center of the detector to the point of intersection of the photon with the detector is given by

$$D = -y_c - x_c \tan\gamma$$

where the angle γ is given by

$$\gamma \equiv \alpha + 2\beta.$$

Thus both the photon energy E and the distance D from the center of the detector to the point of detection are given parametrically in terms of the angle α by

$$E = \frac{n\Lambda}{2d\sin(\alpha + \beta)}$$

$$D = \cos\alpha\left[(A - S)\sin\alpha + \left(A + S\tan^2\alpha\right)\cos\alpha\tan(\alpha + 2\beta)\right]$$

where β and A are given by

$$\beta \equiv \tan^{-1}\left[\frac{(S - A)\tan\alpha}{A + S\tan^2\alpha}\right]$$

$$A \equiv \sqrt{R^2 + \left(R^2 - S^2\right)\tan^2\alpha}.$$